

ROCKING WALLS WITH LEAD EXTRUSION DAMPERS PROTECT FORMERLY HOMELESS SENIORS FROM EARTHQUAKE RISKS

Sandesh Aher¹, David Mar¹, Prof. Geoffrey Rodgers²

Mar Structural Design¹; University of Canterbury²

Berkeley, California, USA¹; Christchurch, New Zealand²

Abstract

1296 Shotwell Street is a new nine-story residential building in San Francisco that will provide affordable housing in a structurally resilient building. This enables shelter-in-place for an economically vulnerable population in the event of a major earthquake. The structure has post-tensioned concrete flat plates and concrete shear walls on a mat foundation. The shear walls are designed to rock during an earthquake, remaining elastic and inducing non-linear flexural responses in the slabs and mat. Gravity loads re-center the shear walls, bringing them back to plumb. Even under the 2,475 year Maximum Considered Earthquake (MCE_R), the shear walls remain elastic. The building was designed based on capacity-design principals. Its performance was vetted using non-linear response-history analysis, with ground motions scaled to the MCE_R hazard level. Resistance to overturning is obtained from superimposed gravity loads, consisting of slab and mat footing self-weight, as well as slab and mat uplift and plastic hinging effects that occur at the ends of the shear walls during rocking and foundation uplift. Where the ends of a shear wall did not have enough restoring strength from the slabs at the building edge, supplemental dampers were provided at the foundation level for additional overturning resistance. The lead extrusion dampers used in this project were developed by Prof. Geoffrey Rodgers from the University of Canterbury in New Zealand. Damage and loss estimates were made for the high-performance design, and compared to a conventional structure, using the Seismic Performance Prediction Program (SP3) tool following FEMA P-58 methodology.

Introduction

1296 Shotwell building is a new senior affordable housing building with 94 units, located in San Francisco, California, with about 20% of the units reserved for the formerly homeless community. It is a 9-story building with a 135' x 75' footprint. The typical floor is around 8,500 sq. ft. The typical story height is 8'-8", while the first story is 14'-0" tall. There are outdoor patios on the second, eighth and ninth floors. The second floor also has an independently supported outdoor area that supports a vegetated roof. There is a mechanical penthouse at the roof. The roof supports solar panels, and mechanical and window washing equipment. Exterior architectural elements include an entrance canopy, entrance sun-shades, roof sunshades and metal screens on south wall.

The gravity framing consists of two-way post-tensioned (PT) and mild steel reinforced slabs spanning to concrete columns that bear on a concrete mat foundation. The building's primary lateral resisting system is cantilevered reinforced concrete shear walls bearing on the mat foundation. Under lower seismic motions, the building's shear walls resist overturning with an essentially fixed base. Under greater seismic excitation, the shear walls rock back and forth, inelastically deforming the elevated and mat slabs. Overturning resistance comes from wall, mat foundation weight, and slab dead loads, bearing on soil under the mat foundation at the ends of the shear wall.

In the inelastic range, the walls and mat foundation rock in stable overturning about the toe at the end of the shear wall under the mat foundation. The strength of the slabs and the mat is activated in the longitudinal direction. In the transverse direction, the supplemental lead dampers are activated in addition

to the slabs and the mat. Mat foundation rocking and hinging was selected as the primary mechanism rather than conventional plastic hinging in the shear wall. The architectural rendering of the building and the Perform analysis model is shown in Figure 1.

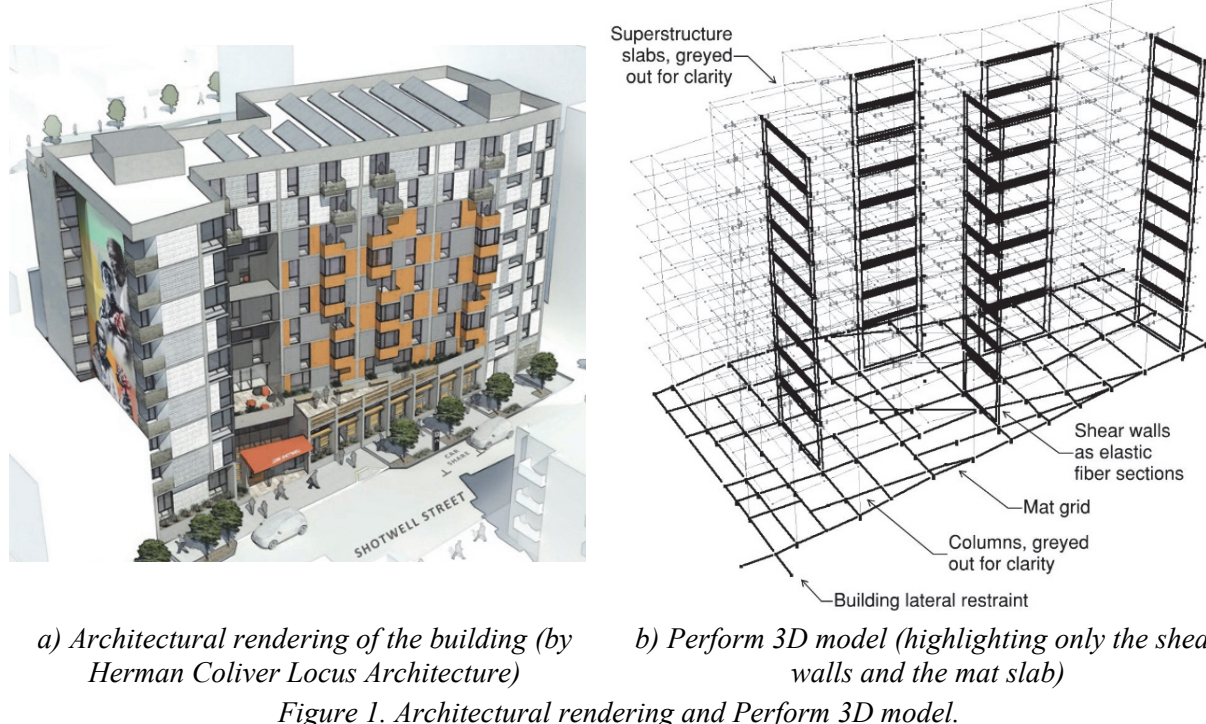


Figure 1. Architectural rendering and Perform 3D model.

Design Approach

Design Criteria. The lateral design of the building followed the Tall Buildings Initiatives (TBI) Guidelines for Performance Based Seismic design of Tall Buildings. Non-linear time history analyses with expected loads and expected material strengths were carried out at both the 43-year Service Level Earthquake (SLE) and the 2,475-year MCE_R event. 11 ground motions were selected and scaled generally following the procedures outlined in Chapter 16 of ASCE 7-16 and Chapter 3 of the TBI Guidelines.

Design of the Mat slab. The mat slab was modeled as a grid of mat strips with tributary concrete cross-section properties, see Figure 2a. The top and the bottom reinforcement in the mat slab was modeled as negative and positive plastic hinges at the ends of the mat strips. The backbone curves for the plastic hinges included expected strengths, strain hardening and cyclic degradation. The mat slab was designed using capacity-based design principles to stay ductile under flexural demands without shear failure. The mat top and bottom reinforcement was designed to yield and dissipate energy during rocking-induced hinging. This reinforcement was proportioned to allow the mat to rock and yield without making the mat slab too strong. The mat reinforcement was iteratively designed until low residual were obtained under the non-linear time-history analysis. This involved a strategy of carefully balancing the shear walls' plan center of strength and rigidity so that plan torsion was minimized. The percentage contribution of the mat to the building strength was about 60-70%. Mat slab bottom reinforcement was designed to distribute the compression loads to the soil below under dynamic seismic loading. Localized ground improvement was specified to achieve a higher soil pressure strength underneath the shear walls than the rest of the mat slab. Tightly spaced shear ties were provided in the mat slab near the shear wall end boundary elements to avoid a two-way punching shear failure. Lightly spaced shear ties in the general area around the shear

walls distributed loads to a broader area of the mat. The mat strips from the Perform model were designed for one-way shear and shear ties were added where required. The mat slab reinforcement away from the shear walls was designed by applying the demands from Perform analysis into a RAM Concept model and performing an elastic analysis. The mat slab at the damper locations and at the block-out for the elevator pit was capacity-based designed using concrete strut and tie principles. The maximum hinge rotations in the mat slab were checked for an acceptance criteria similar to an elevated slab hinge rotation. Ductile ASTM A706 reinforcement was specified for the project. Higher strength Grade 80 reinforcement and T1 and T2 heads were specified where required by analysis. Shear ties in the mat slab were specified with 180-degree hooks on top and T1 heads at the bottom for ease of installation. The embedded pipes and conduits in the mat slab were coordinated with the different disciplines and located in the middle half of the mat, well away from the footprints of the rocking shear walls.

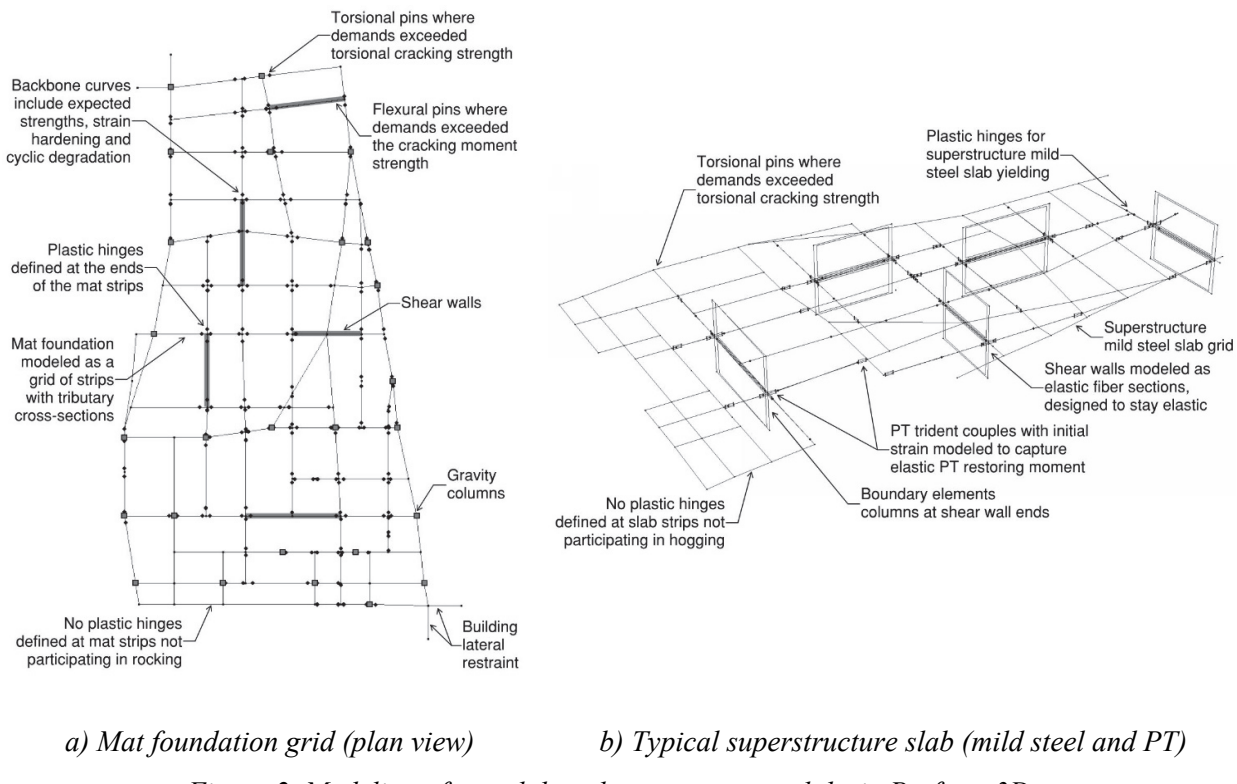


Figure 2. Modeling of mat slab and superstructure slabs in Perform 3D.

Design of the Superstructure Slabs. Gravity design of the elevated PT slabs was done using RAM Concept. For the lateral building strength contribution of the superstructure slabs, a grid similar to the mat slab was modeled in Perform using tributary cross-section properties, see Figure 2b. The superstructure mild steel reinforcement was modeled as plastic hinges with expected strengths, strain hardening and cyclic degradation. The effect of the post-tensioning was captured using a trident couple as shown in Figure 3. The trident consisted of non-linear gap elements at the ends of the shear wall that open and close during building rocking. This creates a moment couple based on the eccentricity of the axial PT force. The axial PT force was applied as an initial strain in the linear elastic bar elements in between the tridents at the beginning of the time-history analysis. The contribution from the superstructure slabs was found to be about 20-25% of the building strength. The shear capacity of the superstructure slabs adjacent the shear walls were designed for $2M_p/L$ of the slab capacity for one-way shear during slab uplift and hinging. Slab-column and slab-wall connections were detailed to accommodate the MCE_R drifts and rocking without punching shear failure, using stud rail reinforcement. Diaphragms were designed to carry

and transfer story shears to the shear walls. Chord and collector reinforcing was provided where needed to resist and transfer the lateral story loads. Maximum hinge rotations in the superstructure slabs were checked against limits per test results from Megally and Ghali, 2000.

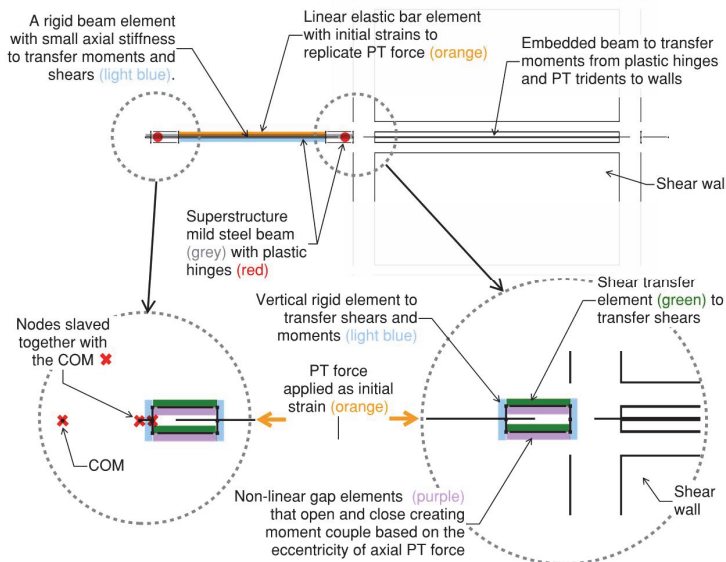


Figure 3. PT trident couple definition

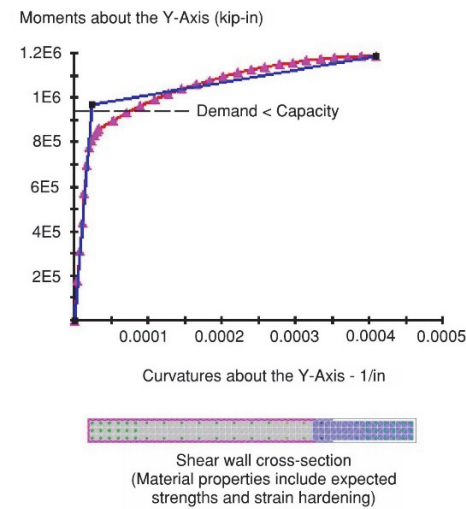


Figure 4. Shear wall design

Design of the Shear Walls. The shear walls were modeled and analyzed as elastic fiber sections in the Perform model and were designed to stay essentially elastic under flexure for demands from the time-history analysis. In the event the mat slab was unexpectedly stronger than what was analyzed and designed for, the shear walls were capacity-based designed to force a flexural plastic hinge at the first story, by keeping the flexure DCRs at that story in the range of 90-95%, see Figure 4. Type 2 couplers were specified at shear wall boundary element vertical reinforcement along the height of the building and at the shear wall web vertical reinforcement dowels into the mat slab at the first story. T-heads were used to anchor the shear wall vertical web and boundary reinforcement into the mat slab. Boundary element ties were partially or fully extended into the mat slab, depending on the location to the edge of the mat. Shear keys and dowels were provided at the shear wall-mat slab interface to transfer shear forces into the mat.

Design of Gravity Columns. Gravity loads for the design of the columns was obtained from an ETABS model. These loads were applied as point loads in the Perform model. Seismic loads for the design of the columns were obtained from time-history analysis in Perform. Columns were designed to accommodate MCE_R drifts without loss of gravity load capacity under axial, bending and shear demands. Typical column tie size and spacing over the full column height were capacity-based designed in shear for 2Mp/L of the column longitudinal reinforcement.

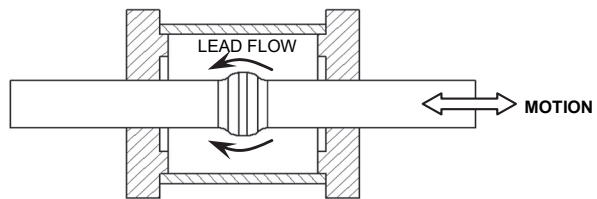
Design of Seismic Piers and Soil improvements. The site was improved using a grid of closely spaced Drilled Displacement Columns (DDCs) to prevent soil liquefaction and lateral spreading. Seismic piers and soil improvements were designed to bear reactions from the structure. Axial reinforcing in the seismic piers were capacity designed in tension to develop the damper forces.

Damper Reaction Mechanics. Lead-extrusion based damping devices were first considered in the 1970s as a method to absorb earthquake response energy during an earthquake in a controlled manner. This creates repeatable hysteretic behavior in a compact package (Robinson and Greenbank 1975; Robinson and Greenbank 1976). The concept is broadly similar to the use of the lead core that provides added energy dissipation in lead-rubber bearings used in base isolation. Historically, these devices have been volumetrically very large and have been used for energy dissipation in structural applications including base isolation (Cousins and Porritt 1993). Figure 5a presents a photograph from Cousins and Porritt (1993), which shows devices with force capacities of 100 and 700kN, and a person to indicate scale. These devices are quite large, but are suitable for the applications previously considered, since the space available was typically not tightly restricted.

Lead extrusion dampers provide a resistive force by plastically extruding the solid lead working material through an orifice created by an annular restriction. Bulged-shaft extrusion dampers utilize a streamlined bulge on the central shaft to create the orifice. A cross-sectional schematic of the bulged-shaft design is presented in Figure 5b.



a) Lead extrusion devices developed for base-isolation applications with 100 and 700 kN force capacities. (Cousins and Porritt 1993)



b) schematic diagram showing how plastic extrusion of lead occurred through an annular orifice

Figure 5. Details of the lead-extrusion damper concept.

The lead-extrusion dampers exhibit a weak velocity dependence, where the damping force produced within the device can be expressed by:

$$F = C_\alpha \dot{x}^\alpha \quad (1)$$

where F = the extrusion damper force; \dot{x} = velocity of the shaft; α = velocity coefficient (constant); and C_α = damper constant determined by physical dimensions/design of the damper (constant for any specific damper design).

Damper Modeling. The damper was modeled in Perform as a yielding link in parallel with a non-linear gap element over soil springs, see Figure 6. The backbone curve for the damper was obtained from damper test results, and is similar to that shown in Figure 9b. Figure 7 shows the assembly of the damper.

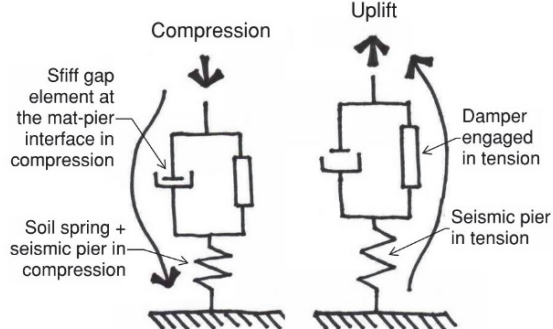


Figure 6. Damper modeling in Perform 3D

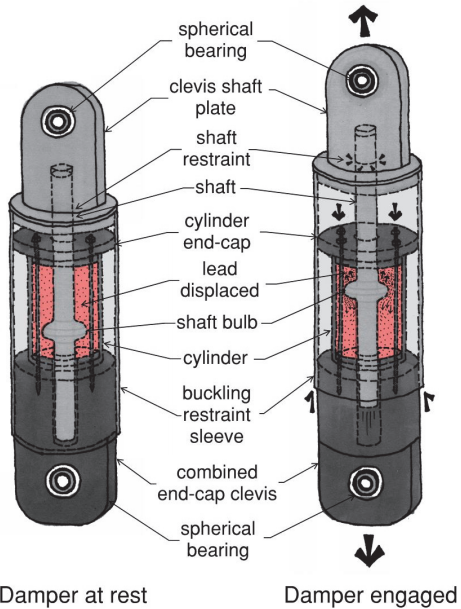


Figure 7. Damper assembly

Specific Damper Design. Modelling of the structure using Perform software indicated that the damper displacement demand during the Service Level earthquake had an average displacement of 0.8 inch and a maximum displacement across all service level ground motions of 1.3 inches. During the Maximum Considered Event (MCE_R), the average damper displacement demand was 4.94 inches and the largest displacement from all eleven MCE_R ground motions considered was 9.45 inches. The damper was designed to have a stroke capacity of 9.5 inches and a nominal design force of 225 kip (1,000kN). Testing was undertaken on the full damper assembly in the same configuration as it was to be installed in the structure. The damper was mounted vertically between two pin connections to closely represent the loading conditions in service. Figure 8a presents a photograph of the damper assembly mounted within the 450kip (2,000kN) capacity Servotest universal test machine.

The Servotest machine controller is capable of producing sine wave displacement profiles. The in-service damper displacement profile will be one-directional, as the damper will extend during uplift and contract again during re-seating of the mat slab. The design incorporates 9.45" (240mm) of extension displacement capacity and approximately 0.8" (20mm) of contraction displacement capacity. These displacement capacity measurements are in reference to the "neutral" position of the damper, at the point where the pin centre-to-centre length is 40" (1016mm).

It was determined that the test machine controller was not capable of doing extension and contraction (cosine) wave inputs from the neutral position of the damper, due to a limitation in the maximum allowable excursion from the initial reference position. Therefore, during the set-up, the damper was first extended by 4.725" (120mm) into its "central" or "mid-stroke" position, from which it has a displacement capacity of $\pm 4.725"$ ($\pm 120\text{mm}$). This amplitude corresponds to a peak-to-peak displacement of 9.45" (240mm). The damper was subjected to five fully-reversed sinusoidal displacement cycles to investigate the influence of heating effects during cyclic loading, see Figure 9a. While some force reduction was observed during the five cycles of loading, this loss of force is temporary and will be recovered once the device cools following an earthquake. This input displacement regime also represents five reversed cycles

at the largest displacement amplitude from all MCE_R ground motions considered during the structural modelling, so this is a very demanding test of the damper behavior.

Overall, the results were consistent across all four dampers, with very similar peak response forces. The maximum force across the five cycles varied from approximately 116% to 88% of the average peak force from the five cycles. The overlay of the hysteretic response of all four dampers subjected to the five cycles is presented in Figure 9b. The damper connections to the clevis plate assembly in the mat slab were capacity designed for the damper force to ensure the connections remain elastic. Waterproofing details at the damper were coordinated with the waterproofing consultant to allow for the mat uplift at the piers at the dampers. Figure 8b shows the installation of the damper at the construction site.

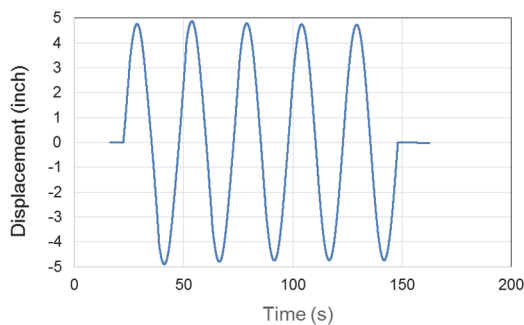


a) Photograph of the damper mounted within the universal test machine during testing.

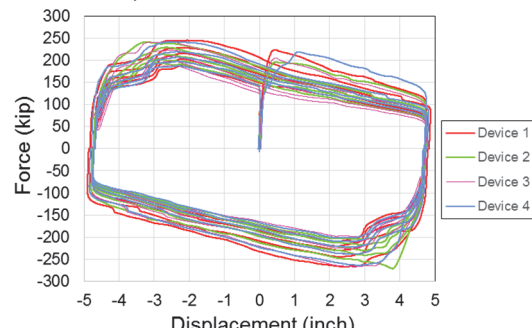


b) Photograph of the damper being installed at the construction site.

Figure 8. Photographs of the damper being tested in the laboratory and installed at the construction site.



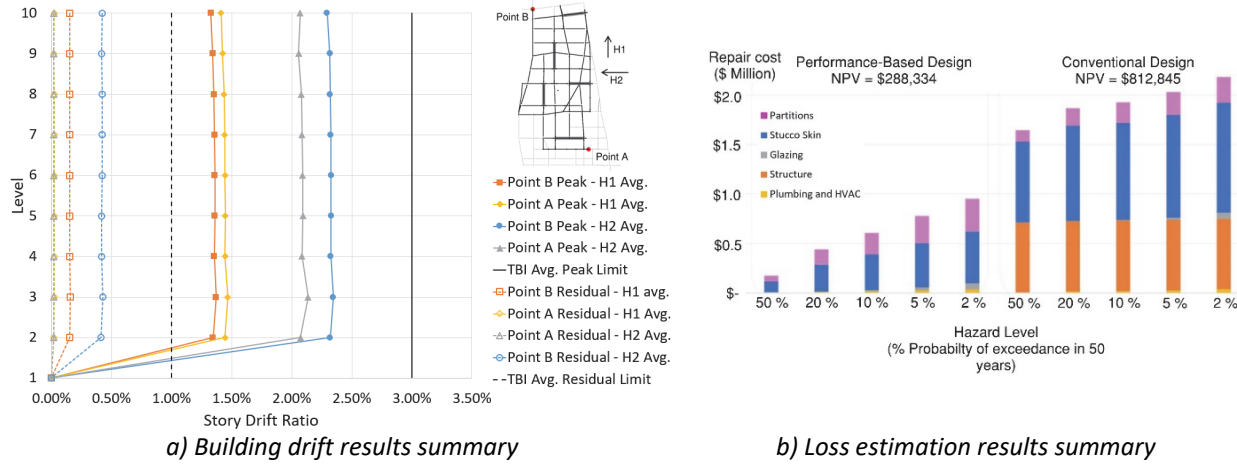
a) Recorded displacement profile – five cycles at $\pm 4.725\text{in}$ at 0.03979Hz



b) Overlay of the hysteretic response of the four dampers when subjected to the input loading protocol in Fig. 9a

Figure 9. An overlay of the hysteresis results from all four dampers subjected to five cycles at 0.0398Hz .

Results Summary. The average MCE_R peak transient story drift ratios were 1.5% and 2.4% in the building longitudinal and transverse directions respectively, see Figure 10a. The average MCE_R residual story drift ratios in those directions were 0.2% and 0.4%. The building drifts satisfied the average and maximum, peak and residual drift limits from the TBI Guidelines for the MCE_R and service level earthquakes. The peak drifts are modest and the low residual drifts demonstrate effective re-centering of the building, enabling shelter-in-place after an earthquake.



a) Building drift results summary

b) Loss estimation results summary

Figure 10. Building drift results summary.

Loss Estimation Summary. Seismic damage and loss estimates were made for the current high-performance design, and compared to a conventional structure with plastic hinges in the shear walls. The Seismic Performance Prediction Program (SP3) tool was used, based on FEMA P-58 methodology. The costs to repair both structural and non-structure components, under a wide range of earthquake events, are considered. The graphical summary in Figure 10b shows that the post-earthquake repair costs of the rocking shear wall performance-based design are much lower than that of a conventional cantilevered shear wall design.

Acknowledgements. The authors would like to thank Prof. Greg Deierlein, Stanford University for providing a very thoughtful peer review of this project.

References

- Cousins, W. J., and Porritt, T. E., 1993, "Improvements to lead-extrusion damper technology." Bulletin of the New Zealand National Society for Earthquake Engineering, 26(3), 342-348.
- Robinson, W. H., and Greenbank, L. R., 1976, "Extrusion Energy Absorber Suitable For The Protection Of Structures During An Earthquake." Earthquake Engineering & Structural Dynamics, 4(3), 251-259.
- Rodgers GW., 2009 "Next Generation Structural Technologies: Implementing High Force-To-Volume Energy Absorbers" PhD thesis, University of Canterbury, Christchurch, New Zealand.
<http://hdl.handle.net/10092/2906>
- Rodgers GW., Chase JG., Heaton D. and Cleeve L., 2013, "Testing of Lead Extrusion Damping Devices Undergoing Representative Earthquake Velocities." New Zealand Society of Earthquake Engineers Annual Conference (NZSEE 2013), Wellington, New Zealand, 26-28 April,
http://www.nzsee.org.nz/db/2013/Poster_47.pdf
- Megally, S., Ghali, A., 2000, "Punching Shear Design of Earthquake-Resistant Slab-Column Connections," *ACI Structural Journal* 97(5), 12 pages.
- Pacific Earthquake Engineering Center (PEER), May 2017, "Tall Buildings Initiative (TBI) Guidelines for Performance-Based Seismic Design of Tall Buildings, Version 2.03."